Surface Modification of PVDF Membranes with Sulfobetaine Polymers for a Stably Anti-Protein-Fouling Performance

Qian Li, Bo Zhou, Qiu-Yan Bi, Xiao-Lin Wang

Department of Chemical Engineering, Membrane Technology and Engineering Research Center, Tsinghua University, Beijing 100084, China

Received 4 November 2011; accepted 21 December 2011
DOI 10.1002/app.36715
Published online in Wiley Online Library (wileyonlinelibrary.com).

ABSTRACT: Two sulfobetaine-based zwitterionic monomers, including 3-(methacryloylamino) propyl-dimethyl-(3-sulfopropyl) ammonium hydroxide (MPDSAH) and 2-(methacryloyloxyethyl) ethyl-dimethyl-(3-sulfopropyl) ammonium (MEDSA) were successfully grafted from poly(vinylidene fluoride) (PVDF) hollow fiber membrane outside surface via chemical activation and atom transfer radical polymerization (ATRP). The ATRP time at 2 h under the 2 mol/L of zwitterionic monomers was the minimum period for the complete coverage of grafted sulfobetaine polymers on the PVDF membrane surface. The surface hydrophilicity of the sulfobetaine-modified PVDF membranes was significantly enhanced. The poly-MPDSAH-*g*-PVDF (GA: 247 $\mu g/cm^2$) and poly-MEDSA-*g*-PVDF membranes (GA: 338 $\mu g/cm^2$) efficiently resisted to the adsorption of both negative and positive charged proteins, and showed excellent anti-protein-fouling performance with flux recovery ratio (RFR) higher than 90% and total fouling (RT) less than 25% during the cyclic filtration of bovine serum albumin solution. After cleaned in membrane cleaning solution for 12 days, the grafted MPDSAH layer on PVDF membrane could maintain without change, however, the poly-MEDSA-*g*-PVDF membrane lost the grafted MEDSA layer. Therefore, the amide group of sulfobetaine, which made a great contribution to the higher hydrophilicity and stability, was significant in modifying the PVDF membrane for a stably anti-protein-fouling performance. © 2012 Wiley Periodicals, Inc. J Appl Polym Sci 000: 000–000, 2012

Key words: poly(vinylidene fluoride); membrane; sulfobetaine; surface modification; anti-protein-fouling performance; stability

INTRODUCTION

Polyvinylidene fluoride (PVDF) has been recognized as one of the most attractive polymers in membrane industry and wildly used in many separation applications because of the extraordinary mechanical property, high chemical resistance, and good thermal stability.[1,2] However, due to the low-surface energy and hydrophobic characteristics, PVDF membranes probably suffer from membrane protein-fouling when used in the practical applications such as biological effluent treatment, protein purification, bacteria filtration, etc.[3] Protein adsorption (PA) on the membrane surface has been considered to be the first step of membrane fouling.[4] The protein-fouling of membranes is often followed by bacterial infection, thrombus formation, and other undesirable reactions and responses.[4,5] Therefore, great importance has been attached to prepare the PVDF membrane with a PA-resistant property. One of the appropriate methods is the surface modification of PVDF membrane.[6]

The poly(ethylene glycol) (PEG)-based materials are commonly used as the antifouling materials for resisting PA, with which the modified surfaces can resist the close approach of biomacromolecules.[7] Ademovic et al.[8] produced a biocompatible PVDF films with a minimization of PA by grafting PEG on the PVDF films. Unfortunately, as a polyether, PEG is susceptible to oxidative degradation and chain cleavage in aqueous systems.[3] In the past decades, a promising alternative zwitterionic nonfouling material has been found which contains both positive and negative charged units.[4,9] The materials containing zwitterionic phosphorylcholine (PC) head-groups have become the representatives to create nonbiofouling surfaces from 1990s, but phosphorylcholine based monomers, such as 2-methacryloyloxy-ethyl phosphorylcholine (MPC), are moisture sensitive and not easy to be synthesized.[10–12] Recently, sulfobetaine, a kind of zwitterionic material with a

Correspondence to: X.-L. Wang (xl-wang@tsinghua.edu.cn).

Contract grant sponsor: National High-tech R&D Program of China (863 Program); contract grant number: 2009AA062901.

Contract grant sponsor: National Program on Key Basic Research Project (973 Program); contract grant number: 2009CB623401.

similar structure of PC, has been proved a biocompatible material with an excellent PA-resistant property.[13,14] Sulfobetaine surfaces are capable of binding a significant amount of water molecules because of the formation of a hydration layer via electrostatic interaction and hydrogen bond.[9,11] Therefore, sulfobetaine can lead to a strong repulsive force to protein at specific separation distances and make the protein contact with the surface in a reverse manner without a significant conformation change.[3,4,11] During the past 5 years, many researchers have confirmed the ability of sulfobetaine coatings on various polymer membranes to resist PA and then significantly retard bacterial biofilm formation.[3,9,11,15–18]

In this research, the surface-initiated atom transfer radical polymerization (ATRP) is frequently used in surface modification because of its main ability to synthesize well-defined polymers in a controlled manner.[12,16,19] Due to the inertness of PVDF, the surface modification of PVDF membranes with sulfobetaine often includes two steps. Generally, PVDF membrane surface should be pretreated to provide active sites or groups for the following ATRP. Chiang modified PVDF membrane surface with sulfobetaine methacrylate (SBMA) via ozone surface activation and ATRP.[3] For the membrane grafted with 0.4 μg/cm^2 of sulfobetaine methacrylate polymer (poly-SBMA), no BSA and little γ-globulin were adsorbed. The flux recovery of the PVDF membrane increased from 28.3% to 88.9% after the first cycle of BSA solution filtration. However, it has been acknowledged that ozonation is an expensive technique due to the unstability of ozone generator and the ATRP process in their work took as long as 24 h.[3,20] Additionally, the comparison of different sulfobetaine-modified PVDF membranes has not been reported and the stability of the grafted sulfobetaine layer on the PVDF membrane surface was never discussed in the previous literatures.

In this work, the specific objective is to synthesize a stably antifouling PVDF hollow fiber membrane with the proper sulfobetaine material. Two typical sulfobetaine monomers, 3-(methacryloylamino) propyl-dimethyl-(3-sulfopropyl) ammonium hydroxide (MPDSAH) and 2-(methacryloyloxyethyl) ethyl-dimethyl-(3-sulfopropyl) ammonium (MEDSA) were grafted from the PVDF hollow fiber membrane surface, respectively. The chemical activation followed by ATRP was applied because it is a relatively economical process and the chemically modified surfaces are stable and efficient.[21] By using the ATRP method, the grating amount (GA) of zwitterionic polymer was controlled. The hydrophilicity and stability of poly-MPDSAH-*g*-PVDF and poly-MEDSA-*g*-PVDF membranes were compared under the same conditions. The surface composition, morphology, and hydrophilicity of the nascent and modified PVDF membranes were characterized by attenuated total reflectance spectrophotometer (ATR-FTIR), X-ray photoelectron spectroscopy (XPS), scanning electron microscope (SEM), and contact angle (CA) meter. The antifouling property was estimated by PA and cyclic filtration. The stability of the modified PVDF membranes was evaluated by monitoring the surface composition and anti-protein-fouling performance during the membrane cleaning.

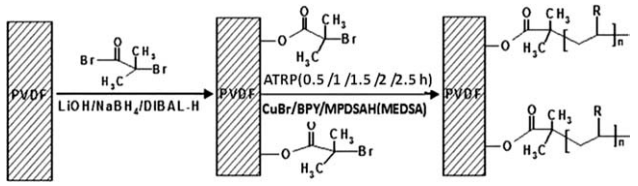

Figure 1 Schematic diagram for fabrication of poly-MPDSAH-*g*-PVDF membrane and poly-MEDSA-*g*-PVDF membrane (R=MPDSAH/MEDSA).

MATERIALS AND METHODS

Materials

A PVDF hollow fiber membrane with an average pore diameter of 0.15 μm and an porosity of 70% was prepared with thermally induced phase separation (TIPS) method. 2,2-Bipyridine (BPY), copper (I) bromide (CuBr), diisobutylaluminium hydride (DIBAL-H, 1.0 mol/L solution in toluene), sodium borohydride ($NaBH_4$), sodium hypochlorite (NaClO), sodium dihydrogen phosphate ($NaH_2PO_4{\cdot}2H_2O$), disodium hydrogen phosphate ($Na_2HPO_4{\cdot}12H_2O$), bovine serum albumin (BSA; $pI = 4.8$, $M_w = 66{,}000$), lysozyme (Lys; $pI = 11.0$, $M_w = 144{,}000$, >20,000 U/mg), and coomassie brilliant blue G250 were purchased from Sinopharm Chemical Reagent Beijing Co., Ltd. (Beijing, China). Lithium hydroxide monohydrate ($LiOH{\cdot}H_2O$), hydrogen chloride (HCl), ethanol, ethane, hexane, pyridine, methanol, 2-propanol, toluene, diethyl ether, and sodium hydroxide (NaOH) were supplied by facility division of Tsinghua University (Beijing, China). 2-bromoisobutyrate bromide (BIBB), 2-(methacryloyloxyethyl) ethyl-dimethyl-(3-sulfopropyl)-ammonium (MEDSA), and 3-(methacryloylamino) propyl-dimethyl-(3-sulfopropyl) ammonium hydroxide (MPDSAH) were favored by Beijing Hengye Zhongyuan Chemical Co., Ltd (Beijing, China). All of reagents were used as received.

Preparation of poly-MPDSAH-*g*-PVDF and poly-MEDSA-*g*-PVDF membrane

The fabrication of poly-MPDSAH-*g*-PVDF and poly-MEDSA-*g*-PVDF membranes is shown in Figure 1. First, the PVDF hollow fiber membranes were immersed into a solution of $LiOH{\cdot}H_2O$ (1.8 mol/L)

in water. The solution was kept at 80°C and stirred. After 24 h of reaction, the samples were removed and rinsed successively with water and 2-propanol, and then dried under vacuum. The treated membranes were immersed into a solution of $NaBH_4$ (0.078 mol/L) in 2-propanol. The solution was maintained at room temperature and stirred for 24 h. After the reaction, the samples were removed and rinsed successively with 2-propanol, a 1 : 1 (v/v) mixture of HCl and ethanol, and a 1 : 1 (v/v) mixture of acetone and water. After dried under vacuum, the membranes were immersed into a solution of DIBAL-H/toluene (0.104 mol/L) for 65 h at room temperature. The membranes (PVDF-OH) were rinsed successively with hexane, a 1 : 1 (v/v) mixture of HCl and ethanol, a 1 : 1 (v/v) mixture of acetone and water, and then dried under vacuum. Second, the hydroxylated PVDF membranes were added into a solution of pyridine (3 mL) in dry diethyl ether (100 mL), followed by dropwise adding BIBB (4 mL) in dry diethyl ether (60 mL) over 10 min. The reaction mixture was gently stirred at 0°C for 2 h, and then at room temperature for another 14 h. The modified PVDF membranes (PVDF-Br) were removed and washed with ethanol and water. The membranes were then dried under vacuum. Third, the PVDF-Br membranes and CuBr (71 mg, 0.5 mmol) were placed in a thoroughly dry flask. Then a degassed solution of methanol (10 mL) and pure water (10 mL) containing BPY (156 mg, 1.0 mmol) and sulfobetaine monomer (MPDSAH or MEDSA) was transferred into the flask under nitrogen protection and polymerized for different periods including 0.5, 1.0, 1.5, 2.0, and 2.5 h, respectively. After the polymerization, the substrates were thoroughly washed with phosphate-buffered saline (PBS, PH = 7.4), a mixture of $NaH_2PO_4{\cdot}2H_2O$ and $Na_2HPO_4{\cdot}12H_2O$. After water rinse, the modified membranes (poly-MPDSAH-*g*-PVDF and poly-MEDSA-*g*-PVDF membrane) were dried under vacuum and weighed. The grafting amount (GA, μg/cm^2) was calculated by using eq. (1):

$$\mathrm{GA} = \frac{W_1 - W_0}{A} \tag{1}$$

where A represents the outside surface area of PVDF membrane (cm^2), W_0 and W_1 are the weights of the nascent and modified PVDF membrane (μg), respectively. Each result was an average of at least three parallel experiments.

Surface chemical composition

The surface chemical compositions of the nascent and modified PVDF membranes were characterized by using attenuated total reflectance (ATR-FTIR) spectrophotometer (Nicolet 6700, USA) and X-ray photoelectron spectroscopy (XPS). Zinc selenide (ZnSe) was applied as an internal reflection element during the ATR-FTIR analyses. Each spectrum was captured by averaged 64 scans at a resolution of 4 cm^{-1}. XPS measurements were performed on a PHI Quantera SXM Scanning X-ray Microprobe (ULVAC-PHI, Japan) with an Al-Mg anode target. The X-ray source was run at 250 W with an electron take off angle of 45° relative to the sample surface. The base pressure of the analyzer chamber was about 5×10^{-7} Pa. The survey scan (from 0 to 1200 eV binding energy range) and the core-lever spectra with much high resolution were both collected. Binding energies were calibrated using the containment carbon (C 1s = 284.6 eV). The data were analyzed using the software package XPS peak 4.1.

Surface morphology

The surface morphologies of the nascent and modified PVDF membranes were observed using a scanning electron microscope (SEM, JSM 7401, JEOL) under standard high-vacuum conditions (1 kV). All the samples were frozen in liquid nitrogen, then deposited on a copper holder and sputtered with gold prior to SEM.

Contact angle measurement

Contact angle (CA) between water and membrane was measured and calculated in static mode on a CA meter (OCA 20, Germany) at 25°C. Water (1 μL) was carefully dropped on the sample surface with an automatic piston syringe and photographed after 100 s. The CA value of each sample was measured at three various positions of one sample.

Protein adsorption

A Bio-Rad Protein Assay was used to evaluate the amount of PA (BSA or Lyz) on the surface of nascent and modified PVDF membranes. Each tested membrane with 20.41 cm^2 of efficient surface area was rinsed with ethanol (20 mL) for 30 min and transferred into a test tube with PBS solution (20 mL, pH = 7.4). After 30 min, the membrane was soaked in protein solutions (1.0 g/L, 5 mL) which were prepared with the PBS solution for 24 h at 37°C. Then, dye reagent containing coomassie brilliant blue G-250 was added into the solutions. Concentration of the solution was determined by the absorbance at 595 nm using a visible-infrared spectrometer. The PA (μg/cm^2) on the membrane could be estimated by using eq. (2).

$$\mathrm{PA} = \frac{(C_0 - C_1) \times V}{A} \tag{2}$$

where C_0 and C_1 are the protein (BSA or Lyz) concentration in PBS solution before and after soaking membrane (μg/mL), V is the volume of soaking solution (mL), and A is the outside surface area of the PVDF membrane (cm^2).

Filtration test

A self-made dead end filtration was applied to characterize the filtration performance of nascent and modified PVDF membranes. BSA was used as a model protein to evaluate the protein resistant characteristics of the membranes under the pressure of 0.1 MPa. Before the test, the membranes were immersed in ethanol for 10 min. First, flux of pure water was determined within 30 min with sampling for every 5 min. The averaged flux was recorded as $J_{v,0}$. Then, two cycles were performed on each tested membrane. In each cycle, a BSA solution (1.0 g/L), prepared by dissolving BSA in the PBS solution, was filtered through the membrane for 2 h until a constant value (noted as $J_{p,i}$), followed by washing the membranes through shaking it in 0.1 mol/L NaOH solution for 30 min and then rinsing it with pure water. After that, flux of pure water was measured again within 30 min and the averaged pure water flux was recorded as $J_{v,i}$ (i indicates the ith cycle). The fluxes ($L/h/m^2$) were obtained by eq. (3).

$$J_{v,i}(J_{p,i}) = \frac{V_i}{A \cdot \Delta t}(i = 0, 1, 2) \tag{3}$$

where V_i, A, and Δt are the permeate volume (L), outside surface area (m^2), and permeation time (h), respectively.

To evaluate the fouling-resistance of a membrane, the relative flux recovery (RFR_i) and the total protein fouling (RT_i) in each cycle of the filtration experiments were calculated by eqs. (4) and (5):

$$\mathrm{RFR}_i(\%) = \frac{J_{v,i}}{J_{v,0}} \times 100(i = 1, 2) \tag{4}$$

$$\mathrm{RT}_i(\%) = \left(1 - \frac{J_{p,i}}{J_{v,i-1}}\right) \times 100(i = 1, 2) \tag{5}$$

The flux loss (RT_i) was caused by both reversible and irreversible protein fouling in each cycle (RR_i and RIR_i). They were defined by eqs. (6) and (7), respectively:

$$\mathrm{RR}_i(\%) = \left(\frac{J_{v,i} - J_{p,i}}{J_{v,i-1}}\right) \times 100(i = 1, 2) \tag{6}$$

$$\mathrm{RIR}_i(\%) = \left(1 - \frac{J_{v,i}}{J_{v,i-1}}\right) \times 100(i = 1, 2) \tag{7}$$

Stability test

The stability of grafted sulfobetaine layer was evaluated by monitoring surface composition and anti-protein-fouling performance of the modified PVDF membrane during the membrane cleaning. Poly-MPDSAH-*g*-PVDF and poly-MEDSA-*g*-PVDF membranes were immersed in 0.5 g/L sodium hypochlorite (NaClO) solution which is usually used for membrane cleaning. After 4, 8, and 12 days, several samples were taken out and rinsed with pure water. Then, the ATR-FTIR supported by CA measurements and the filtration test were applied for the dried samples to identify the changes in the surface composition and anti-protein-fouling performance.

RESULTS AND DISCUSSION

Surface grafting and characterization

In this work, two sulfobetaine monomers (MPDSAH and MEDSA) were grafted from the PVDF hollow fiber membrane surface via chemical activation and ATRP. On the basis of Figure 1, the process of surface modification can be divided into three detailed stages.

The first stage was the generation of hydroxylation on PVDF membrane surface with aqueous $LiOH{\cdot}H_2O$. According to the literature, the dehydrofluorination of PVDF membrane was used by exposure to aqueous $LiOH{\cdot}H_2O$ solution at 80°C.[22,23] In this stage, a hydrogen atom and a fluorine atom were eliminated and an oxygen-containing functionality emerged. The ATR-FTIR absorbance spectra of the nascent and hydroxylated PVDF membranes (PVDF-OH) are shown in Figure 2(a,b). Compared with that of the nascent PVDF membrane surface (PVDF), additional broad band in the range of 3000–3600 cm^{-1} (O—H stretching vibration) could be seen from the spectra of PVDF-OH membrane. The second stage was to immobilize the initiator, BIBB, onto the surface of PVDF membrane by esterification of the hydroxyl groups covalently linked to the surface with BIBB.[24] The characteristic peaks at 3421 cm^{-1} (O—H stretching) disappeared completely in the absorbance spectra of PVDF-Br membrane Fig. 2(c), indicating the conversion of the hydroxyl groups to corresponding esters. The third stage in the preparation process was polymerizing the MPDSAH or MEDSA to the PVDF-Br membrane via ATRP with catalyzing by using Cu(I)/BPY. The typical spectra of the modified PVDF membranes are displayed in Figures 2 and 3. In Figure 2(d), an obvious characteristic peak attributing to the bending vibration of amide I (C=O) and amide II (N—H) which originated from the side chains of poly-MPDSAH appeared at 1646 cm^{-1} and 1533 cm^{-1}, respectively. In Figure 2

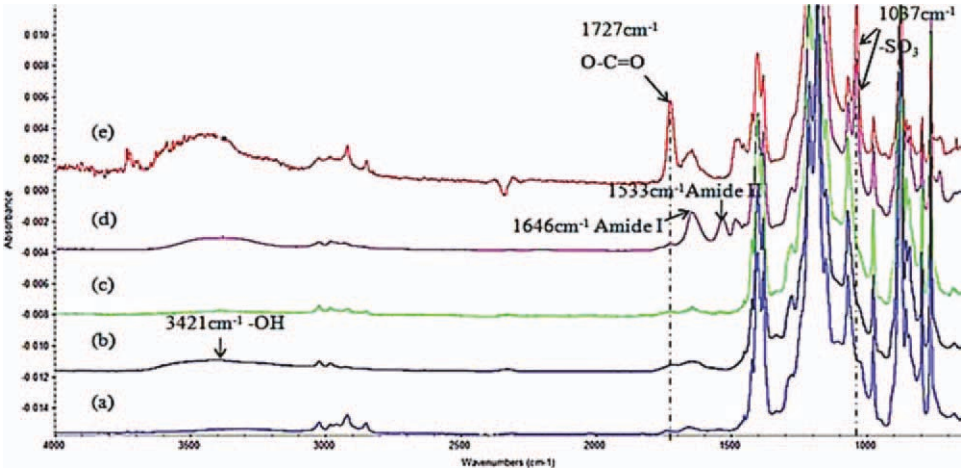

Figure 2 ATR-FTIR spectra of (a) PVDF membrane, (b) PVDF-OH membrane, (c) PVDF-Br membrane, (d) poly-MPDSAH-*g*-PVDF membrane, and (e) poly-MEDSA-*g*-PVDF membrane. [Color figure can be viewed in the online issue, which is available at wileyonlinelibrary.com.]

(e), the adsorption centered at 1727 cm^{-1} (O—C=O stretching) could be seen from the spectra of the poly-MEDSA-*g*-PVDF membrane. Therein, the peaks of both modified PVDF membranes at 3429 cm^{-1} resulted from the adsorbed water in the air. In Figure 2(d,e), a distinct peak attributing to the stretching vibration of —SO^3 group which originated from the side chains of poly-MPDSAH and poly-MEDSA appeared around 1037 cm^{-1}. Moreover, Figure 3(a–d) suggested that the intensity of the characteristic peaks of amide (1646 cm^{-1} and 1533 cm^{-1}) and —SO^3 (1037 cm^{-1}) stretching vibration became stronger with the increase of poly-MPDSAH GA. On the other hand, in Figure 3(a′–d′), the intensity of O—C=O adsorption at 1727 cm^{-1} and —SO^3 at 1037 cm^{-1} obviously increased as the GA of poly-MEDSA increased from 93 μg/cm^2 to 338 μg/cm^2. The chemical compositions of the membrane surfaces were further determined by the XPS analysis. For the nascent PVDF membrane [Fig. 4(a)], two major emissions at 280.1 and 683.4 eV assigned to the binding energy of C 1s and F 1s, respectively. After dehydrofluorination and initiator immobilization on the PVDF membrane, the characteristic peak of F 1s disappeared but the peaks around 69.0 (Br 3d), 182.2 (Br 3p), and 255.2 eV (Br 3s) appeared on the PVDF-Br membrane surface [Fig. 4(b)]. As shown in Figure 4(c,d), the characteristic peaks of S 1s (230.9 eV), S 2p (167.4 eV), N 1s (402.1 eV), and O 1s (527.5 eV) were ascertained from the spectrum of the poly-MPDSAH-modified and poly-MEDSA-modified PVDF membrane surfaces. Supporting information Table I lists the relative element contents measured from XPS analysis for the nascent and modified PVDF membrane surfaces. For the poly-MPDSAH-*g*-PVDF membrane the ratios of N/S were almost 1.0 and for the poly-MEDSA-*g*-PVDF membrane the ratios were almost 2.0, which indicated that sulfobetaine structure was resistant to degradation during the modification process in this work.[11] The results

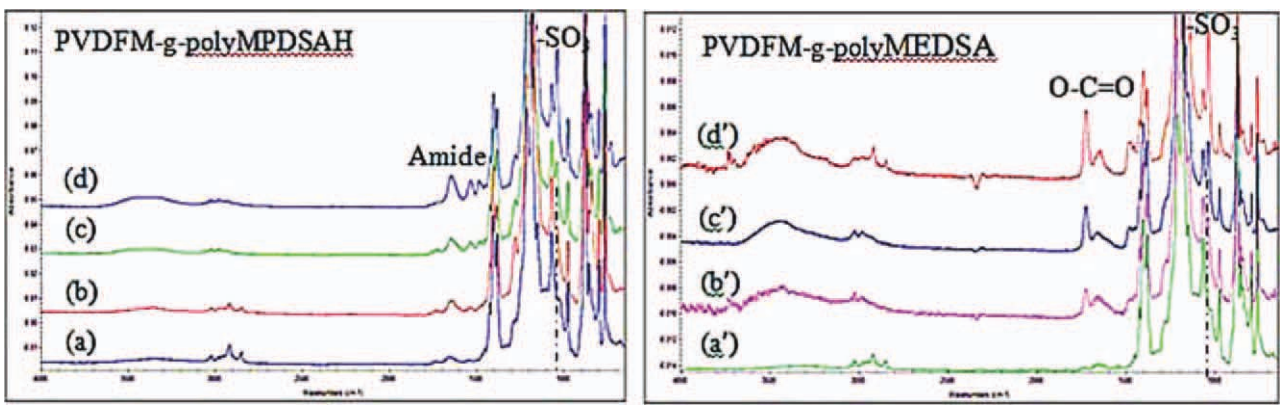

Figure 3 ATR-FTIR spectra of (a and a′) PVDF membrane, poly-MPDSAH-*g*-PVDF membrane with GA of (b) 69 μg/cm^2, (c) 153 μg/cm^2, and (d) 247 μg/cm^2, and poly-MEDSA-*g*-PVDF membrane with GA of (b′) 93 μg/cm^2, (c′) 178 μg/cm^2, and (d′) 338 μg/cm^2. [Color figure can be viewed in the online issue, which is available at wileyonlinelibrary.com.]

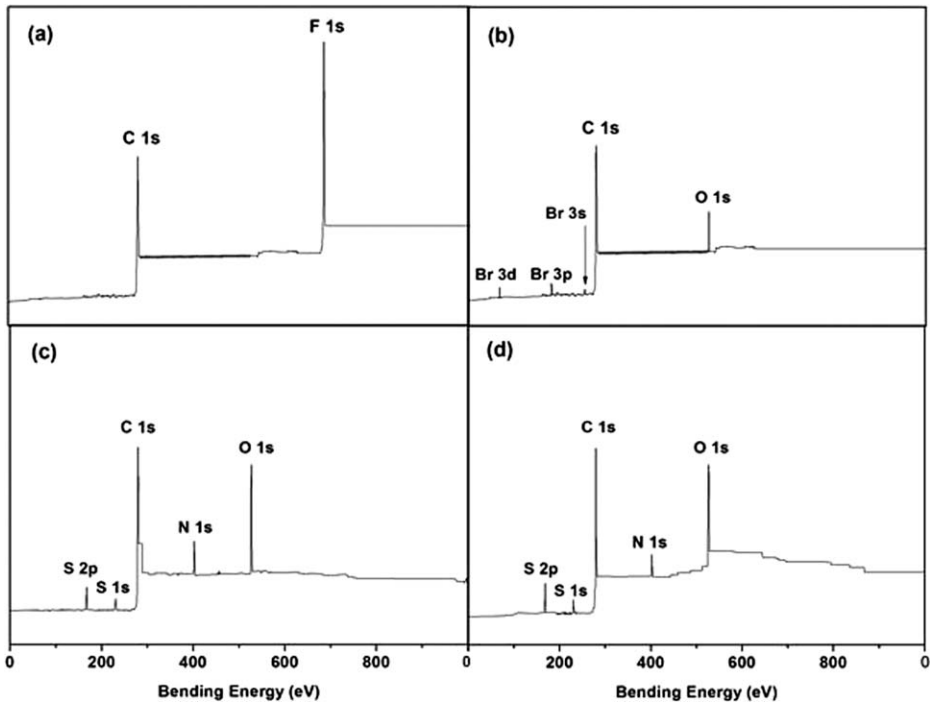

Figure 4 C 1s core-level XPS spectra of (a) PVDF membrane, (b) PVDF-Br membrane, (c) poly-MPDSAH-*g*-PVDF membrane with GA of 247 μg/cm^2, and (d) poly-MEDSA-*g*-PVDF membrane with GA of 338 μg/cm^2.

demonstrated that sulfobetaine layers were successfully fabricated on the outside surface of PVDF hollow fiber membrane in this study.

The GA of poly-MPDSAH and poly-MEDSA can be adjusted with controlling the reaction time of ATRP and the concentration of initial monomer. The GA was measured by the weight increase per area after surface modification [as seen in eq. (1)]. Supporting information Table II shows the dependence of the GA on ATRP time and initial monomer concentration. It could be seen that prolonging the ATRP time increased the GA, while the increase rate of GA slowed down at a long reaction time. All of the GAs increased rapidly at the beginning of ATRP reaction and then leveled off after 1.5 h. In the ATRP reaction stage, water/methanol and CuBr/Bpy complex were used as the solvent and catalyst, respectively. In aqueous media, it is considered that the structure of the catalytic species is a mono-cationic complex $[Cu(I)(Bpy)_2]^+$ with a halide counterion.[18,25] The ionic catalyst species in aqueous media were active enough so that the addition of water in the solvent would increase the polymerization rate. Therefore, a fast growth of the polymerized MPDSAH or MEDSA chains was observed at the beginning of the ATRP reaction. It was also obvious that the GA increased with the increase of sulfobetaine concentration. The increase of monomer concentration caused more chance for surface free radical to contact with the monomers and a higher GA was achieved. When the zwitterionic monomers (MPDSAH or MEDSA) of 2 mol/L was added during the ATRP reaction for 2 h, the GA values of poly-MPDSAH-*g*-PVDF and poly-MEDSA-*g*-PVDF membrane were 247 μg/cm^2 and 338 μg/cm^2, respectively. The values of the GA can be comparable with the results of other's study on the sulfobetaine-modified PVDF membranes, but the period of ATRP process in our work was much shorter than that in the previous study.[3]

Morphological and hydrophilic characterization

The surface and cross-section morphologies of the PVDF membranes before and after modifying were examined by SEM, as shown in Figure 5. Compared with the nascent PVDF membrane [Fig. 5(a)], the opening of the most pores at the modified membrane surfaces appeared to be significantly reduced because the zwitterionic polymer chains covered them after ATRP reaction. It could be observed in Figure 5(b,d) that the poly-MPDSAH-*g*-PVDF membrane with GA of 115 μg/cm^2 and the poly-MEDSA-*g*-PVDF membrane with GA of 124 μg/cm^2 were only partially covered with grafted zwitterionic polymers. As the GA increased to 247 μg/cm^2 and 338 μg/cm^2, respectively, the pores on membrane surface looked being fully covered [Fig. 5(c,e)]. No differences were found between the nascent and modified PVDF membranes in the outer cross-section morphologies, thus, the modification showed no effect on the cross-section morphology of the PVDF hollow fiber membrane.

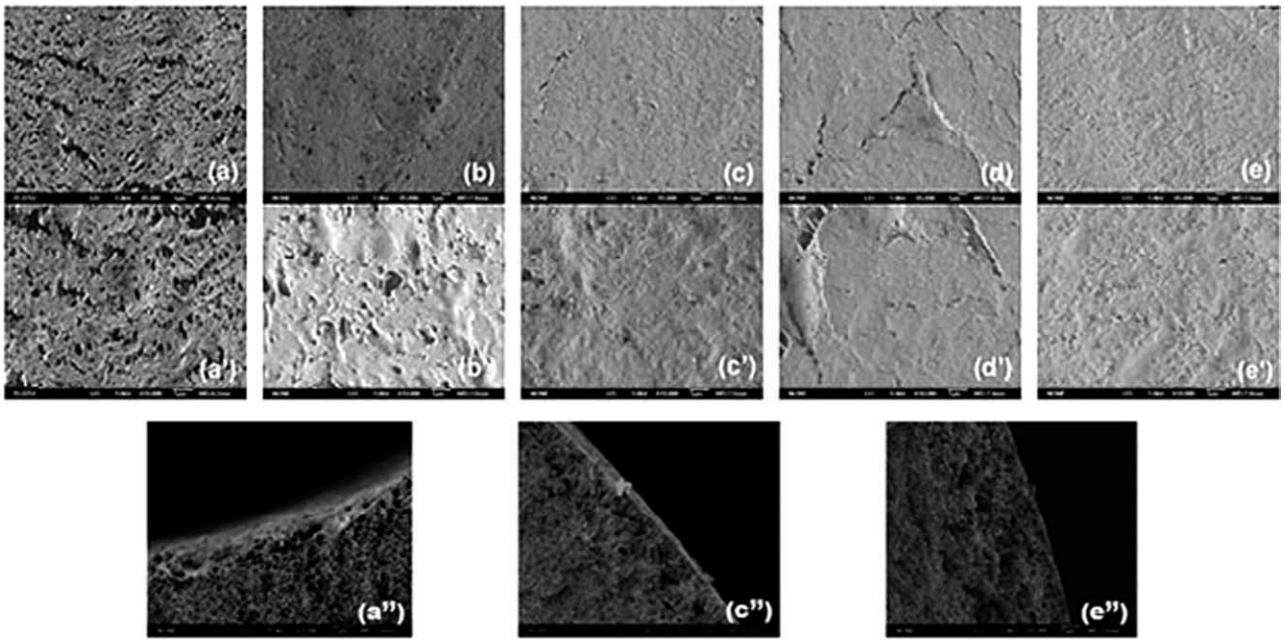

Figure 5 SEM images of (a, a′, and a") PVDF membrane, poly-MPDSAH-*g*-PVDF membrane with GA of (b and b′) 115 μg/cm^2 and (c, c′ and c") 247 μg/cm^2, poly-MEDSA-*g*-PVDF membrane with GA of (d and d′) 124 μg/cm^2 and (e, e′ and e") 338 μg/cm^2 (upside: outside surface, magnification is ×5000; middle: outside surface, magnification is ×10,000; downside: outer cross-section, magnification is ×1000)

The surface hydrophilicity as one of the important properties can affect the flux and antifouling ability of membranes.[11,18] In this work, the CA values of the modified membranes were measured to confirm the formation of poly-MPDSAH and poly-MEDSA on the PVDF membrane and to assess the hydrophilization effect of grafted sulfobetaine polymers. Figure 6 shows the dependence of static CA on the GA of sulfobetaine polymers. On the one hand, due to the intrinsic hydrophobicity of PVDF, the CA of the nascent PVDF membrane was as high as 75.9°. After grafting with sulfobetaine polymers, the CA values decreased due to the successful grafting of zwitterionic sulfobetaine polymers from the chemically inert PVDF membrane surface. On the other hand, the CA dropped below 15° and 40° when the GA of poly-MPDSAH and poly-MEDSA reached 247 μg/cm^2 and 338 μg/cm^2, respectively. Further increasing the GA, the CA values of poly-MPDSAH-*g*-PVDF membrane and poly-MEDSA-*g*-PVDF membrane were almost constant. It indicated that as GA reached 247 μg/cm^2 the grafted poly-MPDSAH completely covered PVDF membrane surface, so further increasing the GA would make little contribution to the surface hydrophilicity. Similarly, the GA had to reach 338 μg/cm^2 for the complete covering of the

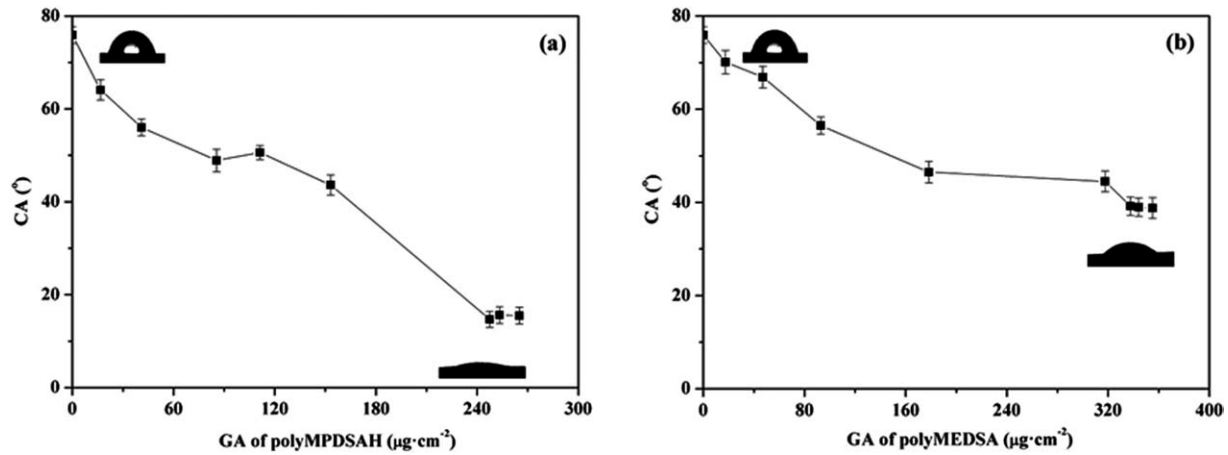

Figure 6 Contact angle of the modified PVDF membrane with different GA values. (a) poly-MPDSAH-*g*-PVDF membrane; (b) poly-MEDSA-*g*-PVDF membrane.

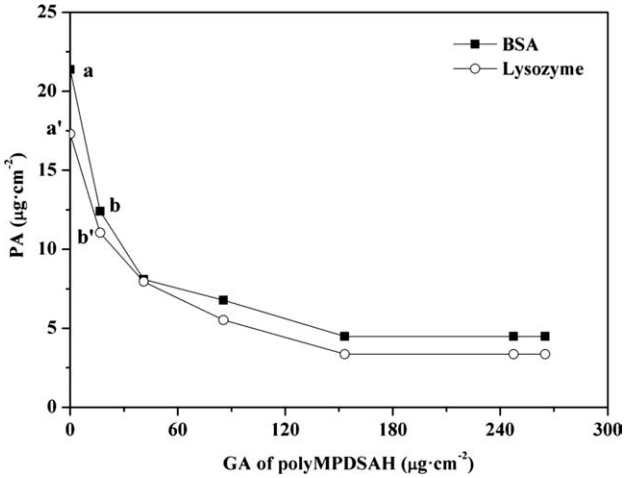

Figure 7 Protein adsorption of poly-MPDSAH-*g*-PVDF membrane with different GA values.

poly-MEDSA-*g*-PVDF membrane surface. The results were consistent to that of the surface morphology. Besides, it could be found that the hydrophilicity of poly-MPDSAH-*g*-PVDF membrane was superior to that of poly-MEDSA-*g*-PVDF membrane. It was attributed to the additional hydrophilic amide group (O═C─NH) in the molecular structure of MPDSAH, which can be seen in Supporting information Table III.

Anti-protein-fouling performance

Protein adsorption

The antifouling property of the modified PVDF membranes was evaluated by testing the adsorption and filtration performance for two major proteins, including BSA and Lyz. In the experiment (pH = 7.4), BSA was negatively charged ($\xi \approx 22.3$ mV) and Lyz was positively charged ($\xi \approx 3.5$ mV).[26] The PA was evaluated by incubating the membranes in the protein solution, and the amount of adsorbed protein was estimated by measuring the reduced protein concentration through Bio-Rad Protein Assay.

Figure 7 shows the effects of GA on the BSA or Lyz adsorption. The adsorption of BSA and Lyz on the nascent PVDF membrane was 21 μg/cm^2 and 17 μg/cm^2 respectively. Differently, a hydration layer was formed on the poly-MPDSAH-grafted membrane, which was believed to play an important role in surface resistance to the protein fouling. It could be found that the adsorption of either BSA or Lyz on the modified PVDF membrane with poly-MPDSAH (Point a or a′) was one-half of that on the nascent PVDF membrane surface (Point b or b′). MPDSAH maintains a overall charge neutrality, hence, no significant difference was found in the adsorption of negatively and positively charged proteins (i.e., BSA and Lyz). As increasing the GA of poly-MPDSAH, the PA decreased until a constant level. PA is affected by numerous factors of surface including surface charge, surface topology, chemistry of the surface, and so on.[27,28] As seen in Figure 5, the small pores on the surface of poly-MPDSAH-*g*-PVDF membrane were blocked when GA was increased to 247 μg/cm^2, thus the effect of GA on PA was decreased. Figure 8 compares the PA of the various membranes. Compared with the nascent PVDF membrane, the protein adsorption of the modified PVDF membranes was inhibited. Figure 9 shows the SEM images of the three surfaces after incubating in protein solution for 3 h. As shown in Figure 9(a), several protein macromolecules were adhered on the nascent PVDF membrane surface. However, after the surface-initiated ATRP of zwitterionic polymers on PVDF membrane, few proteins were found on the modified PVDF membranes [Fig. 9(b,c)]. The more hydrophilic surfaces have the weaker interaction from the outer layer and possibly from the inner core of protein, and the adsorption of protein is less favorable on the hydrophilic surfaces.[29]

Cyclic filtration of BSA solution

The protein adsorption of a membrane usually demonstrates a good correlation with the membrane performance during protein filtration.[3,11] The functionalization of the modified PVDF membrane surface with MPDSAH or MEDSA in this study has made the PVDF membrane highly hydrophilic and having efficient performance on resisting to the adsorption of protein. To further investigate the anti-protein-fouling performance of the modified PVDF membranes, we carried out the cyclic filtration tests with pure water and BSA solution. The flux decline with

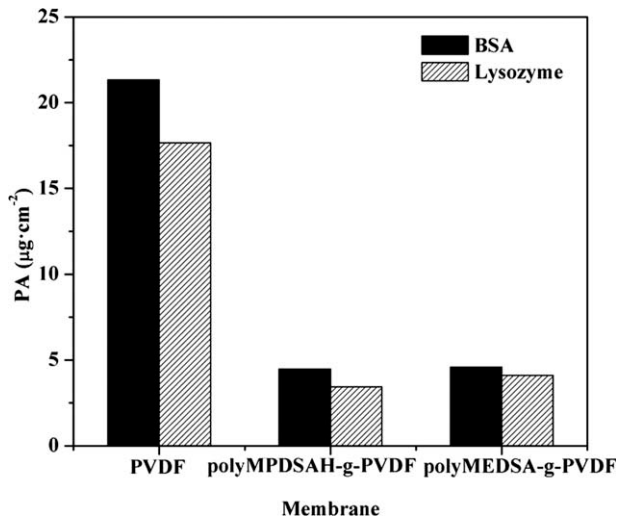

Figure 8 Protein adsorption of PVDF membrane, poly-MPDSAH-*g*-PVDF membrane with GA of 247 μg/cm^2, and poly-MEDSA-*g*-PVDF membrane with GA of 338 μg/cm^2.

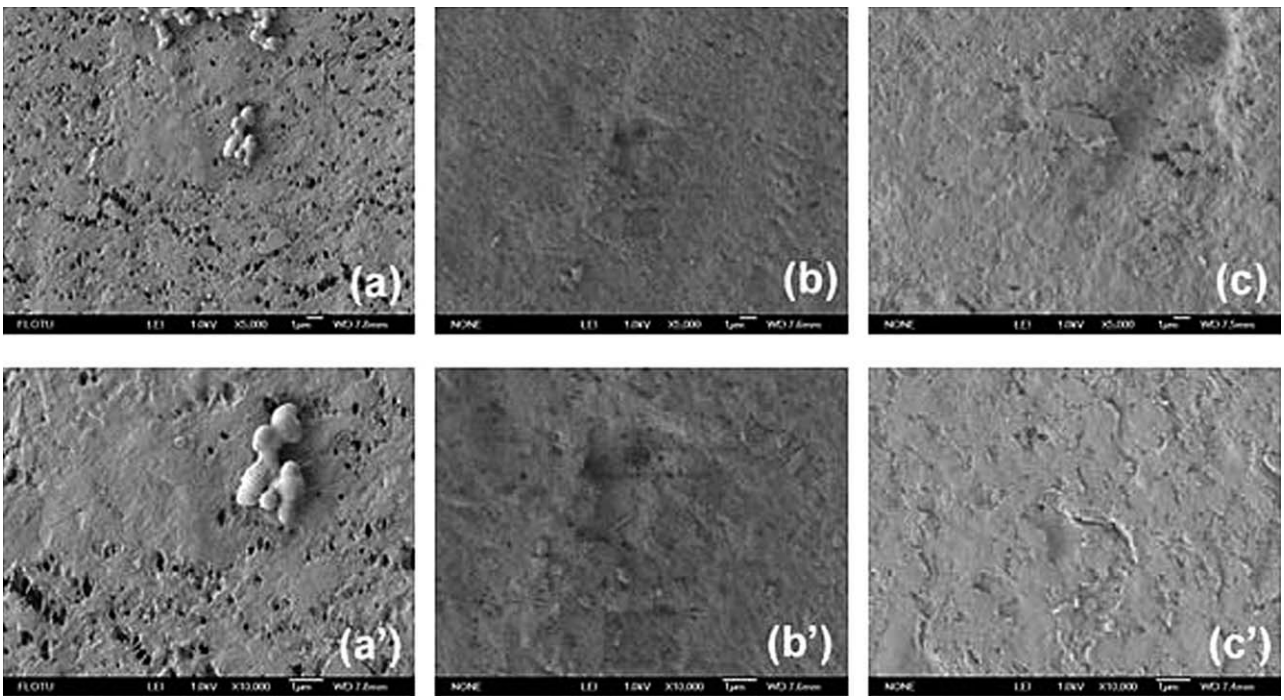

Figure 9 SEM images of (a) PVDF membrane, (b) poly-MPDSAH-*g*-PVDF membrane with GA of 247 μg/cm^2, and (c) poly-MEDSA-*g*-PVDF membrane with GA of 338 μg/cm^2 after incubating in BSA solution for 3 h (upside: magnification is ×5000; downside: magnification is ×10,000).

time, flux recovery and degree of protein fouling were studied in detail.

Before starting the test, each sample was filtrated by pure water at 0.1 MPa for at least 30 min until a steady flux ($J_{v,0}$) was achieved. The effect of GA on $J_{v,0}$ of the poly-MPDSAH-*g*-PVDF membrane is shown in Figure 10(a). The $J_{v,0}$ of nascent PVDF membrane was 1592 L/h/m^2. A slight increase of $J_{v,0}$ was observed when the PVDF membrane was grafted by poly-MPDSAH. It was attributed to the improvement of surface hydrophilicity. The flux of poly-MPDSAH-*g*-PVDF membrane with GA of 41.0 μg/cm^2 was increased to 1641 L/h/m^2 and $J_{v,0}$ was almost constant with further enhancing the GA. As the value of GA exceeded 247 μg/cm^2 $J_{v,0}$ was decreased. It could be ascribed to the decrease of pore size caused by the crowded poly-MPDSAH chains. The results indicated that the contribution of GA to the additional hydraulic resistance outweighed that to the improved hydrophilicity when the GA was higher than 247 μg/cm^2. Combined with the above results, it could be concluded that the ATRP time at 2 h under the 2 mol/L of sulfobetaine monomer (the GA of 247 μg/cm^2, as seen in Table I) was a minimum for the complete coverage of grafted poly-MPDSAH on PVDF membrane

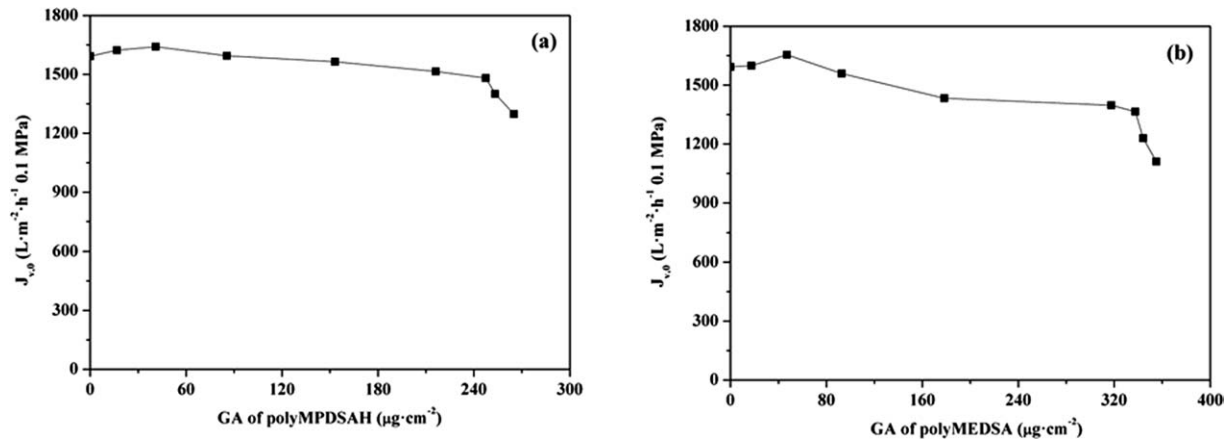

Figure 10 Pure water fluxes of the modified PVDF membranes with different GA values. (a) poly-MPDSAH-*g*-PVDF membrane; (b) poly-MEDSA-*g*-PVDF membrane.

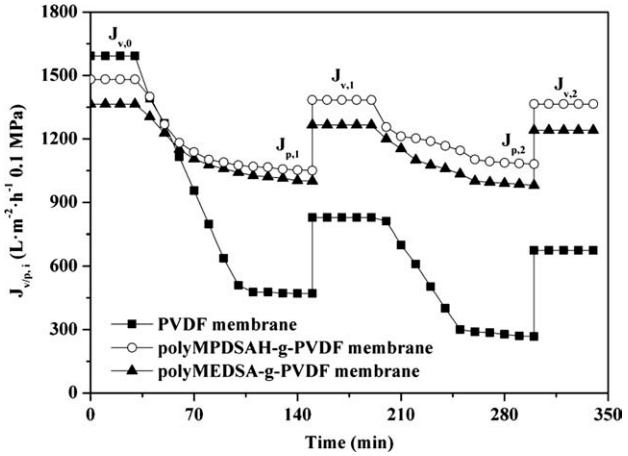

Figure 11 Permeate flux decline behavior of PVDF membrane, poly-MPDSAH-*g*-PVDF membrane with GA of 247 μg/cm^2, and poly-MEDSA-*g*-PVDF membrane with GA of 338 μg/cm^2 during the filtration of BSA solution.

surface. As shown in Figure 10(b), $J_{v,0}$ of the poly-MEDSA-*g*-PVDF membrane exhibited a similar result with the GA of 338 μg/cm^2.

Figure 11 shows the permeation fluxes of BSA solution through the nascent and modified PVDF membranes. It could be seen that, for each circle, the permeate fluxes of nascent and modified PVDF membranes declined rapidly at the start of filtration. And the relatively steady permeation fluxes ($J_{p,i}$) were finally observed at the later stage of each filtration circle, suggesting that the adsorption/deposition and the back diffusion of the protein molecules reached an equilibration at the membrane surface. It was observed that the modified PVDF membranes with MPDSAH and MEDSA exhibited a much slow flux decline with time and the final steady permeate fluxes of them were much higher than that of the nascent PVDF membrane. The results indicated that the grafting of poly-MPDSAH or poly-MEDSA chain efficiently reduced the degree of flux decline caused by protein fouling on the PVDF membrane. Besides, the permeate flux decline of poly-MPDSAH-*g*-PVDF membrane exhibited smaller than that of poly-MEDSA-*g*-PVDF membrane due to the higher hydrophilicity.

In each circle, after the BSA solution filtration, PVDF membranes were washed and then the pure water fluxes [$J_{v,i\ (i\ =\ 1,2)}$] were measured again. The values of $J_{v,i}$ and $J_{p,i}$ could be used to calculate the relative flux recovery (RFR_i) and total fouling (RT_i). The RFR_i defined as the ratio of pure water flux in the *i*th cycle to that in the initial process could reveal the extent of cleaning efficiency and the effect of irreversible fouling resistance of the membrane.[3,17] The higher value of RFR_i indicated the lower persistent protein adsorption to the membrane operated during the *i*th cycle. The RT_i represented the percentage flux loss because of protein adsorption and retention. According to the eq. (5), the lower RT_i meant the membrane could maintain a higher flux in the *i*th cycle of BSA filtration. The loss may be contributed by both persistent protein adsorption and temporal protein blockage which were defined as the reversible fouling ratio (RR_i) and irreversible fouling ratio (RIR_i), respectively. By hydraulic cleaning, the RR_i could be recovered but the RIR_i could not.

It was observed in Figure 12 that the value of RFR_1 was only 52% for the nascent PVDF membrane after the first filtration circle. However, the high values were achieved (more than 90%) when 247 μg/cm^2 of poly-MPDSAH or 338 μg/cm^2 of poly-MEDSA grafted from the PVDF membrane surface. It suggested significant irreversible protein fouling occurred when the nascent PVDF membrane was used, while the modified PVDF membranes prevented the fouling phenomena. The RFR_2 values of two modified PVDF membranes were still high (92.1% and 90.9%, respectively), meaning that only small further fouling occurred after the first cycle. On the contrary, the nascent PVDF membrane showed a decrease in the RFR_2 (42.3%), indicating that irreversible fouling occurred continuously. The values of $RT_{i\ (i\ =\ 1,2)}$ of the modified PVDF membranes were much lower than those of nascent PVDF membrane in both circles, meaning that the modified PVDF membranes could maintain a very low fouling in BSA filtration. The change of protein conformation which was mainly maintained by hydrophobic and hydrogen bonds was one of the driving forces for protein adsorption and the reason of irreversible membrane fouling. In this study, the highly hydrophilic zwitterionic groups of poly-

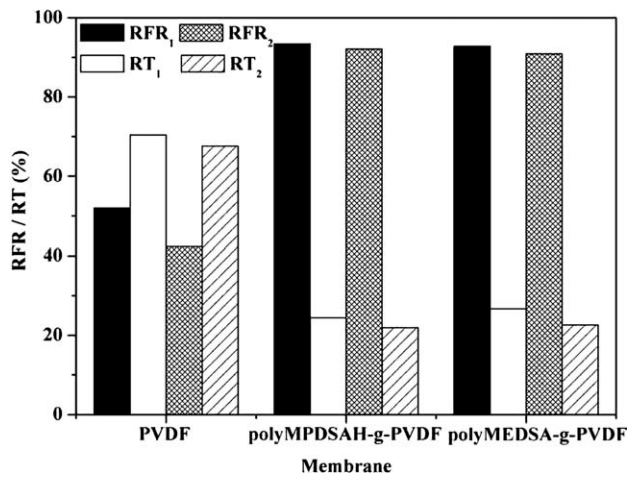

Figure 12 Relative flux recovery ($RFR_{i,\ i\ =\ 1,2}$) and the total fouling ($RT_{i,\ i\ =\ 1,2}$) during the *i*th cycle of PVDF membrane, poly-MPDSAH-*g*-PVDF membrane with GA of 247 μg/cm^2, and poly-MEDSA-*g*-PVDF membrane with GA of 338 μg/cm^2.

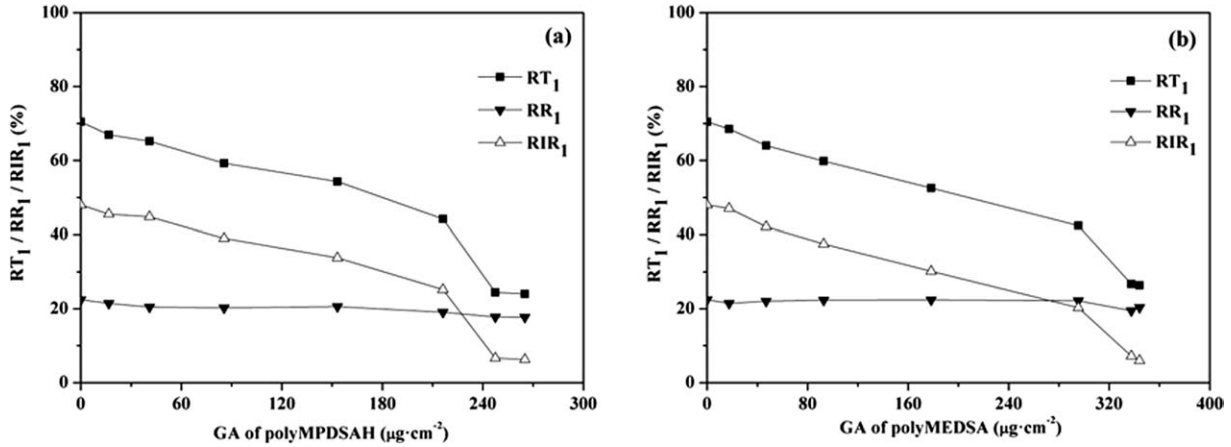

Figure 13 Dependence of RT_1, RR_1, and RIR_1 on GA. (a) poly-MPDSAH-*g*-PVDF membrane; (b) poly-MEDSA-*g*-PVDF membrane.

MPDSAH and poly-MEDSA could take up high portion of free water on the membrane surface and formed a water layer via electrostatic interaction, which provided a steric repulsion as the protein approached to the PVDF membrane surface. Besides, in aqueous medium, the grafting chains with zwitterionic structure cannot diffuse into the interior of protein molecules, while they can minimize the effect on exterior surface ions of proteins, and can maintain the "normal conformation" of protein molecules.[29,30] Therefore, the protein molecule had less chance to contact the modified PVDF membranes than the nascent PVDF membrane. As a result, the modified PVDF membranes exhibited a reduced total membrane fouling, especially irreversible membrane fouling.

To further analyze membrane fouling, the reversible fouling ratio and irreversible fouling ratio in the first-cycle (RR_1 and RIR_1) were discussed in detail. Figure 13(a,b) illustrate the dependence of RT_1, RR_1, and RIR_1 on GA. For the both modified PVDF membranes, poly-MPDSAH-*g*-PVDF and poly-MEDSA-*g*-PVDF membranes, the RT_1 decreased with the increase of GA and a sudden drop of RT_1 occurred at the GA of 247 μg/cm^2 and 338 μg/cm^2, respectively. The RIR_1 had a similar trend to the RT_1 over the GA, however, RR_1 showed a slightly increase with the GA. These results indicated that a part of irreversible fouling converted into the reversible fouling with the increase of GA. As a result, the both modified PVDF membranes could recover a high water flux after hydraulic cleaning. Therefore, the grafting of sulfobetaine polymer on the PVDF membrane efficiently reduced the membrane fouling during the cyclic filtration. The results confirmed that the GA values of 247 μg/cm^2 and 338 μg/cm^2 were the optimum for the poly-MPDSAH-*g*-PVDF and poly-MEDSA-*g*-PVDF membranes, respectively.

Stability

The stability of the grafted polymer layer (poly-MPDSAH or poly-MEDSA) on the PVDF membrane was evaluated in sodium hypochlorite (NaClO) solution which is usually used for membrane cleaning.[31,32] Figure 14 presents the ATR-FTIR absorbance spectra of the poly-MPDSAH-*g*-PVDF and poly-MEDSA-*g*-PVDF membranes after cleaned in NaClO solution for different periods. The ATR-FTIR absorbance for the introduced groups of both modified PVDF membranes, such as O—C=O, amide and —SO^3, did not change when the cleaning time was less than 8 days Fig. 14(a–c, a′–c′). However, when the cleaning time increased to 12 days, as shown in Figure 14(d′), the characteristic peaks of O—C=O and —SO^3 in poly-MEDSA-*g*-PVDF membrane disappeared. The results indicated that the surface composition of poly-MEDSA-*g*-PVDF membrane varied after immersed in NaClO solution for 12 days. To support this result, CA values of the cleaned poly-MPDSAH-*g*-PVDF and poly-MEDSA-*g*-PVDF membranes were measured. Figure 15 displays the images of static water drops on various modified PVDF membranes. The CA values of poly-MPDSAH-*g*-PVDF membrane did not change significantly with the increase of cleaning time. However, it could be observed in Figure 15(a′–d′) that the part of water drop exposed in the air enlarged and the CA values of poly-MEDSA-*g*-PVDF membrane increased with the increase of cleaning time. When cleaned for 12 days, the poly-MEDSA-*g*-PVDF membrane [CA of 72.3°, as shown in Fig. 14(d′)] showed a comparable hydrophobicity with the nascent PVDF membrane [CA of 75.9°, as shown in Fig. 6(a)], which indicated the membrane lost the grafted hydrophilic polymer.

The anti-protein-fouling performance of the membranes after cleaned in sodium hypochlorite solution

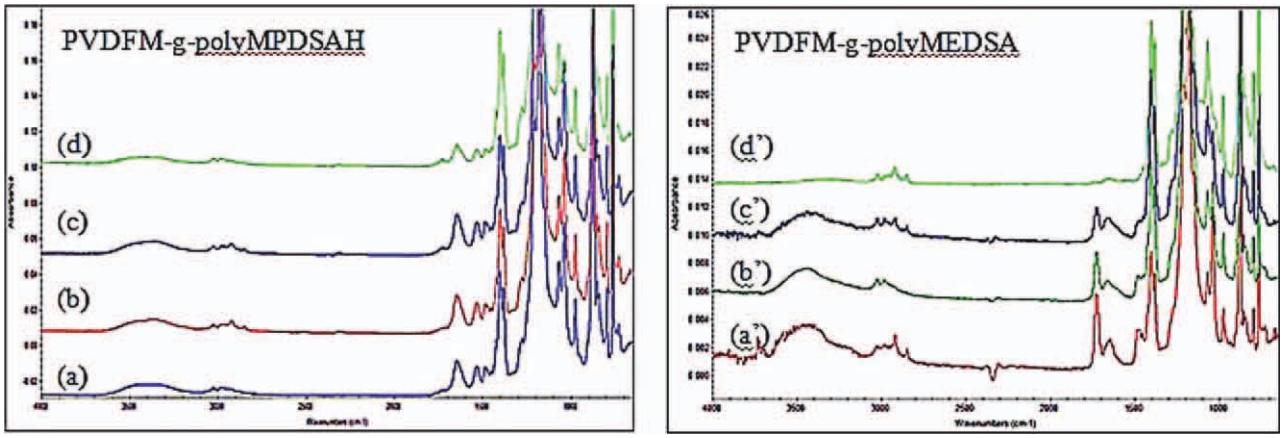

Figure 14 ATR-FTIR spectra of poly-MPDSAH-*g*-PVDF membrane with GA of 247 μg/cm^2 and poly-MEDSA-*g*-PVDF membrane with GA of 338 μg/cm^2 after cleaned in 500 mg/L NaClO solution for (a and a′) 0, (b and b′) 4, (c and c′) 8, and (d and d′) 12 days. [Color figure can be viewed in the online issue, which is available at wileyonlinelibrary.com.]

was studied and illustrated in Figure 16. RFR_1 and RT_1 of poly-MPDSAH-*g*-PVDF membrane remained practically unchanged even cleaning for 12 days. For poly-MEDSA-*g*-PVDF membrane, increasing the cleaning time decreased RFR_1 but increased RT_1, which demonstrated the decline of anti-protein-fouling property.

This study clearly demonstrated that little loss or hydrolysis of the grafted MPDSAH on the poly-MPDSAH-*g*-PVDF membrane occurred within 12 days in cleaning solution. Compared with the poly-MEDSA-*g*-PVDF membrane, the poly-MPDSAH-*g*-PVDF membrane exhibited a much better stability. It can be ascribe to the amide bond in MPDSAH which is more stable than the ester bond in MEDSA.[17,33]

CONCLUSIONS

In this study, a highly hydrophilic and anti-protein-fouling PVDF hollow fiber membrane with a good stability was prepared by chemical activated surface treatment and ATRP process with sulfobetaine monomer. The ATR-FTIR, XPS, and SEM analysis confirmed that the two sulfobetaine polymers (poly-MPDSAH and poly-MEDSA) were successfully grafted from the PVDF membrane. The modified PVDF membrane surfaces became highly hydrophilic, and the amount of protein adsorbed on the PVDF membrane surfaces was reduced to less than a half of that on the nascent PVDF membrane surface. On the basis of the amide group, poly-MPDSAH-*g*-PVDF membrane showed a higher hydrophilicity than poly-MEDSA-*g*-PVDF membrane. When GA values of poly-MPDSAH and poly-MEDSA reached 247 μg/cm^2 and 338 μg/cm^2, respectively, the CA values of both modified PVDF membranes became constant and the $J_{v,0}$ values started to decrease. It could be concluded that the ATRP time at 2 h under the 2 mol/L of zwitterionic monomers was the minimum period for the complete coverage of grafted sulfobetaine polymers on the PVDF membrane surface (the GA values of poly-

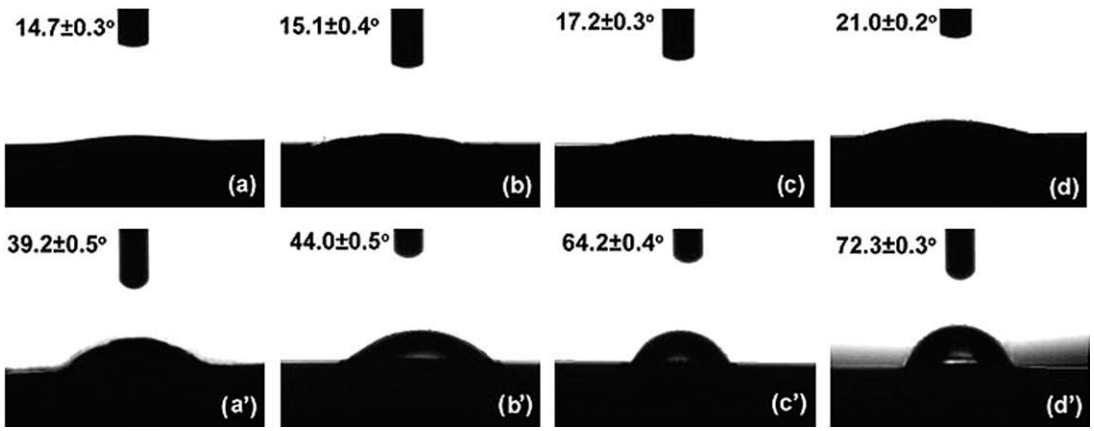

Figure 15 Contact angle and static images of a water drop on poly-MPDSAH-*g*-PVDF membrane with GA of 247 μg/cm^2 and poly-MEDSA-*g*-PVDF membrane with GA of 338 μg/cm^2 after cleaned in 500 mg/L NaClO solution for (a and a′) 0, (b and b′) 4, (c and c′) 8, and (d and d′) 12 days.

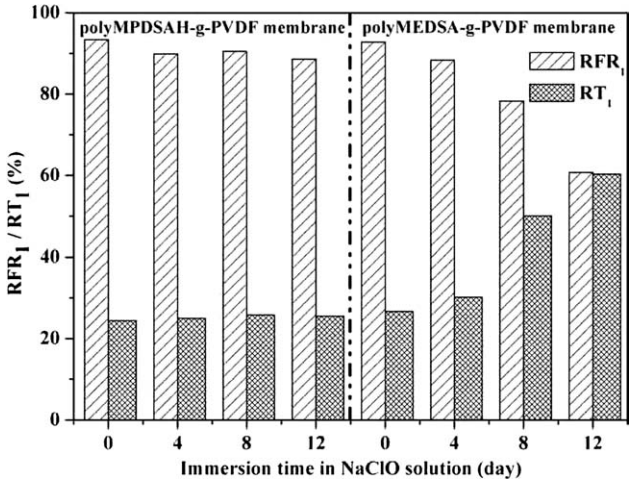

Figure 16 RFR_1 and RT_1 of poly-MPDSAH-*g*-PVDF membrane with GA of 247 μg/cm^2 and poly-MEDSA-*g*-PVDF membrane with GA of 338 μg/cm^2 after cleaned in 500 mg/L NaClO solution for 0, 4, 8, and 12 days.

MPDSAH-*g*-PVDF and poly-MEDSA-*g*-PVDF membrane: 247 μg/cm^2 and 338 μg/cm^2). With conducting the cyclic experiments for BSA solution filtration, the modified PVDF membranes were proved a better anti-protein-fouling performance than the nascent PVDF membrane. The stability of the grafted polymer layers on the surfaces of PVDF membranes was examined by cleaning the membrane samples in NaClO solution. After cleaned for 12 days, the poly-MEDSA-*g*-PVDF membrane lost the grafted polymers and showed a declined anti-protein-fouling performance, however, almost no changes in the surface composition and anti-protein-fouling performance of the poly-MPDSAH-*g*-PVDF membrane were found due to the good chemical stability from the amide group (O═C─NH). Therefore, the amide group of sulfobetaine played an important role in the modification of the PVDF hollow fiber membrane via chemical activation and surface-initial ATRP for the anti-protein-fouling performance with a long-term stability.

References

1. Yang, J.; Li, D. W.; Lin, Y. K.; Wang, X. L.; Tian, F.; Wang, Z. J Appl Polym Sci 2008, 110, 341.
2. Li, Q.; Xu, Z. L.; Yu, L. Y. J Appl Polym Sci 2010, 115, 2277.
3. Chiang, Y. C.; Chang, Y.; Higuchi, A.; Chen, W. Y.; Ruaan, R. C. J Membr Sci 2009, 339, 151.
4. Cho, W. K.; Kong, B. Y.; Choi, I. S. Langmuir 2007, 23, 5678.
5. Seo, J. H.; Matsuno, R.; Konno, T.; Takai, M.; Ishihara, K. Biomaterials 2008, 29, 1367.
6. Liu, F.; Hashim, N. A.; Liu, Y.; Abed, M. R. M.; Li, K. J Membr Sci 2011, 375, 1.
7. Ostuni, E.; Chapman, R. G.; Holmlin, R. E.; Takayama, S.; Whitesides, G. M. Langmuir 2001, 17, 5605.
8. Ademovic, Z.; Klee, D.; Kingshott, P.; Kaufmann, R.; Hocker, H. Biomol Eng 2002, 19, 177.
9. Liu, P. S.; Chen, Q.; Wu, S. S.; Shen, J.; Lin, S. C. J Membr Sci 2010, 350, 387.
10. Xu, Z. K.; Dai, Q. W.; Wu, J.; Huang, X. J.; Yang, Q. Langmuir 2004, 20, 1481.
11. Yang, Y. F.; Li, Y.; Li, Q. L.; Wan, L. S.; Xu, Z. K. J Membr Sci 2010, 362, 255.
12. Zhang, Z.; Chen, S. F.; Chang, Y.; Jiang, S. J. J Phys Chem B 2006, 110, 10799.
13. Yuan, J.; Mao, C.; Zhou, J.; Shen, J.; Lin, S. C.; Zhu, W.; Fang, J. L. Polym Int 2003, 52, 1869.
14. Cheng, G.; Zhang, Z.; Chen, S. F.; Bryers, J. D.; Jiang, S. Y. Biomaterials 2007, 28, 4192.
15. Shan, B.; Yan, H.; Shen, J.;Lin. S. C. J Appl Polym Sci 2006, 101, 3697.
16. Liu, P. S.; Chen, Q.; Liu, X.; Yuan, B.; Wu, S. S.; Shen, J.; Lin, S. C. Biomacromolecules 2009, 10, 2809.
17. Yu, H. J.; Cao, Y. M.; Kang, G. D.; Liu, J. H.; Li, M.; Yuan, Q. J Membr Sci 2009, 342, 6.
18. Zhao, Y. H.; Wee, K. H.; Bai, R. J Membr Sci 2010, 362, 326.
19. Kim, J. B.; Huang, W. X.; Miller, M. D.; Baker, G.; Bruening, M. L. J Polym Sci Part A: Polym Chem 2003, 41, 386.
20. Wojtenko, I.; Stinson, M. K.; Field, R. Crit Rev Environ Sci Technol 2001, 31, 295.
21. Rana, D.; Matsuura, T. Chem Rev 2010, 110, 2448.
22. Chen, Y.; Sun, W.; Deng, Q.; Chen, L. J Polym Sci Part A: Polym Chem 2006, 44, 3071.
23. Marchand-Brynaert, J.; Jongen, N.; Dewez, J. L. J Polym Sci Part A: Polym Chem 1997, 35, 1227.
24. Liu, D. M.; Chen, Y. W.; Zhang, N.; He, X. H. J Membr Sci 2006, 101, 3704.
25. Matyjaszewski, K.; Xia, J. Chem Rev 2001, 101, 2921.
26. Palacio, L.; Ho, C. C.; Pradanos, P.; Hernandez, A.; Zydney, A. L. J Membr Sci 2003, 222, 41.
27. Kung, F. C.; Yang, M. C. Colloid Surf B 2006, 47, 36.
28. Chenoweth, D. E. Ann N Y Acad Sci 1987, 516, 306.
29. Roach, P.; Farrar, D.; Perry, C. C. J Am Chem Soc 2005, 127, 8168.
30. Cheng, N.; Brown, A. A.; Azzaroni, O.; Huck, W. T. S. Macromolecules 2008, 41, 6317.
31. Susanto, H.; Ulbricht, M. Langmuir 2007, 23, 7818.
32. Rouaix, S.; Causeserand, C.; Aimar, P. J Membr Sci 2006, 277, 137.
33. Zalipsky, S. Bioconjugate Chem 1995, 6, 150.